Robust heterostructure of bimetallic sodium–zinc metal–organic framework and reduced graphene oxide for high–performance supercapacitors

Richa Rajak,[a] Mohit Saraf,[b] and Shaikh M. Mobin*[a,b,c]

[a]Discipline of Chemistry, [b]Discipline of Metallurgy Engineering and Materials Science and [c]Discipline Biosciences and Biomedical Engineering, Indian Institute of Technology Indore, Simrol, Khandwa Road, Indore 453552, India

*E-mail: xray@iiti.ac.in
Tel: +91 731 2438 752

Contents:

Fig. S20 (a) Comparison of CV profiles of bare GCE and ***3–GCE*** at 100 mV s^{-1}, (b) CV profiles of ***3–GCE*** at varied scan rates (10–300 mV s^{-1}), (c) GCD plots of ***3–GCE*** at different current densities (1.6–4 A g^{-1}), and (d) plot between specific capacitance and current density. (All results at higher mass loading ~3.5 mg/cm^2)

Table S1. Bond lengths [Å] and angles [°] for **1**.

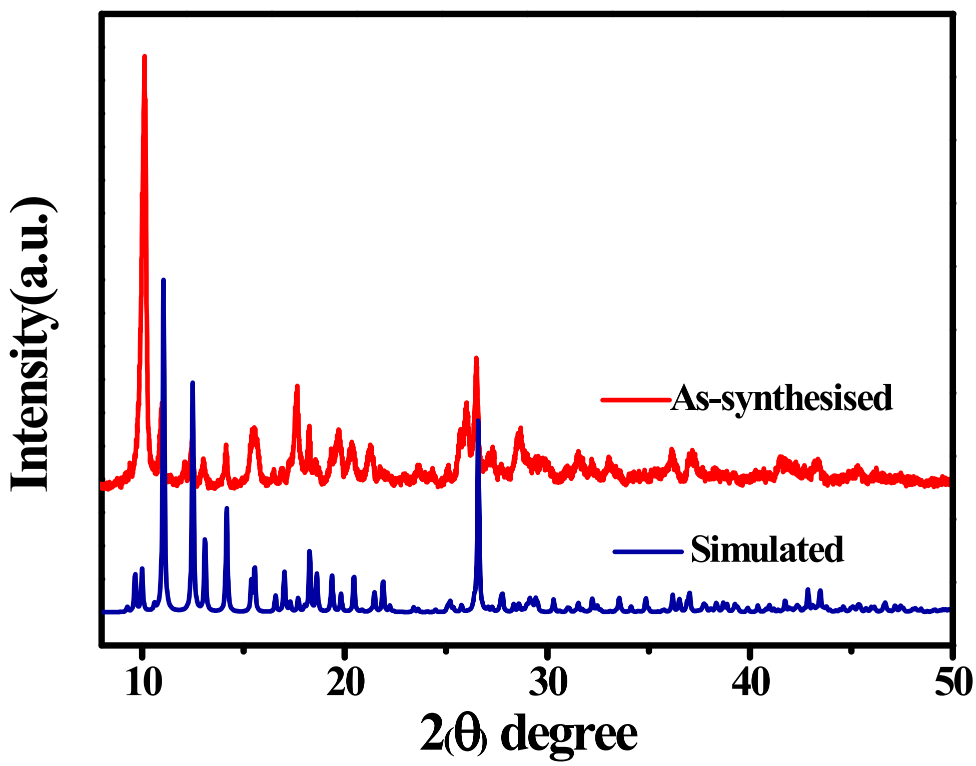

Fig. S1 PXRD spectra of **1**. (Simulated: Blue, As-synthesised: Red)

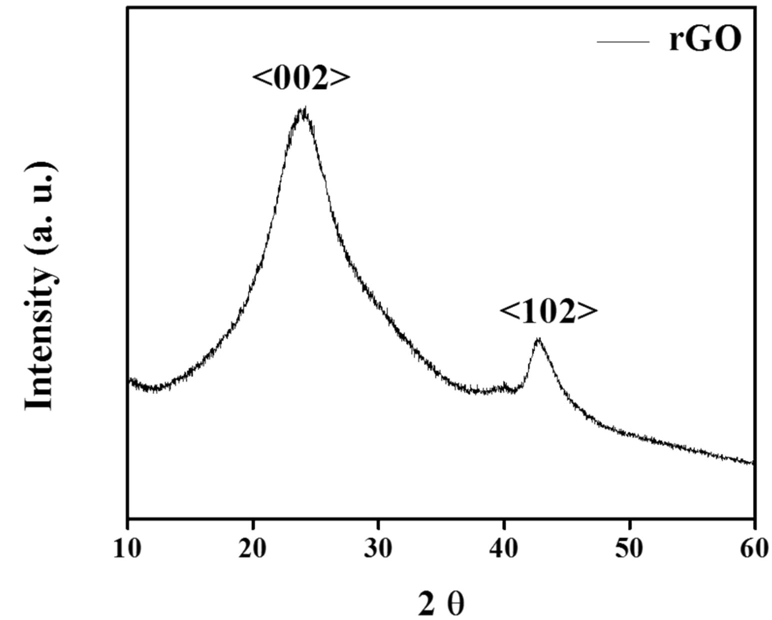

Fig. S2 PXRD of rGO (**2**).

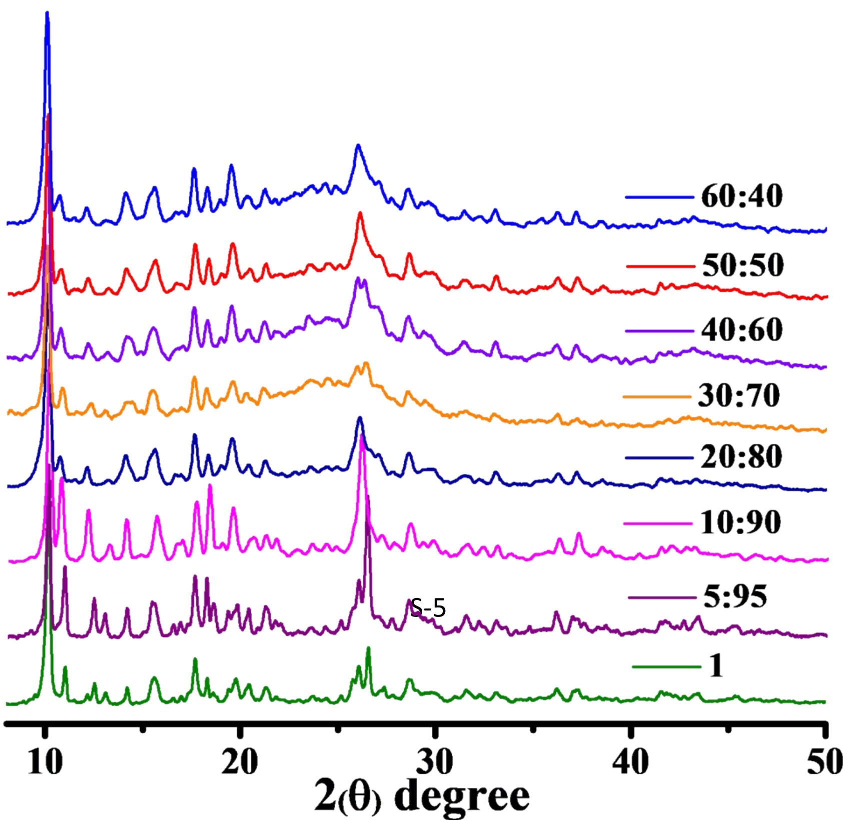

Fig. S3 PXRD spectra of **1** and different heterostructures of **3** formed at different ratio of **1** and **2**. (For e.g. 5:95 indicates 5% of **2** and 95% of **1**, 10:90 indicates 10% of **2** and 90% of **1** and so on...)

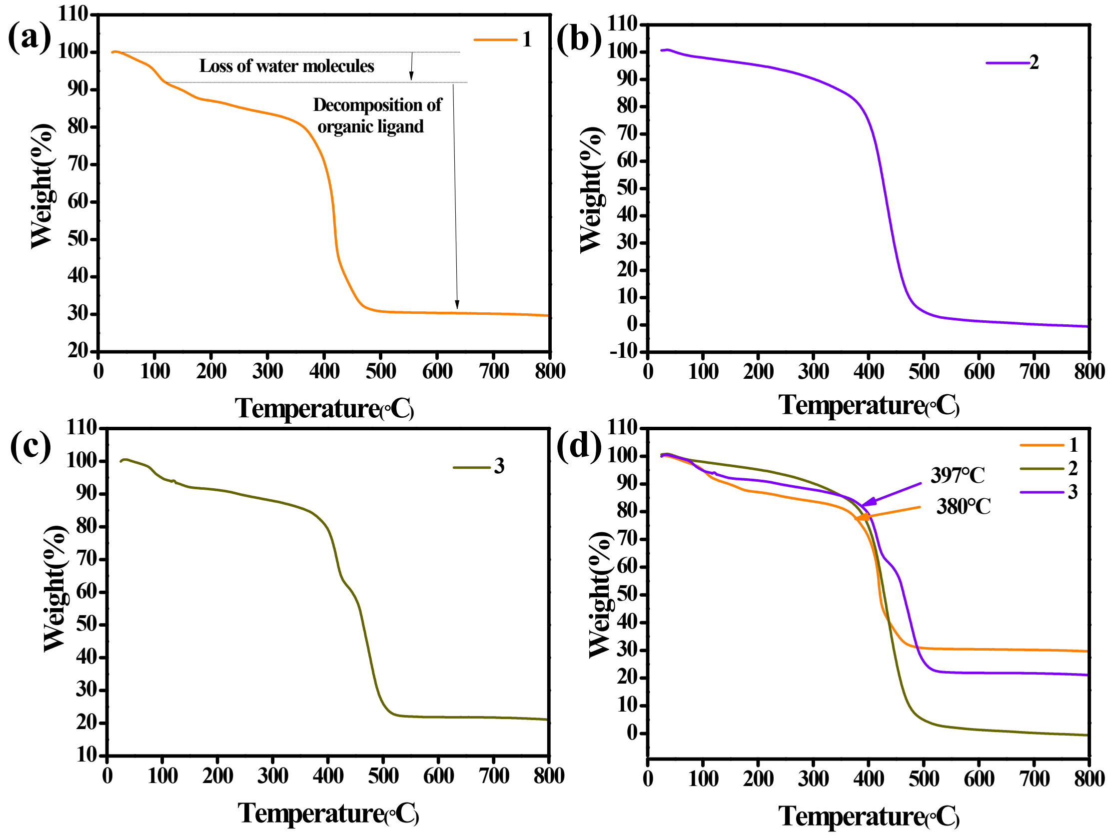

Fig. S4 TGA graphs of **1, 2** and **3** (a-c) separately, and (d) all-together.

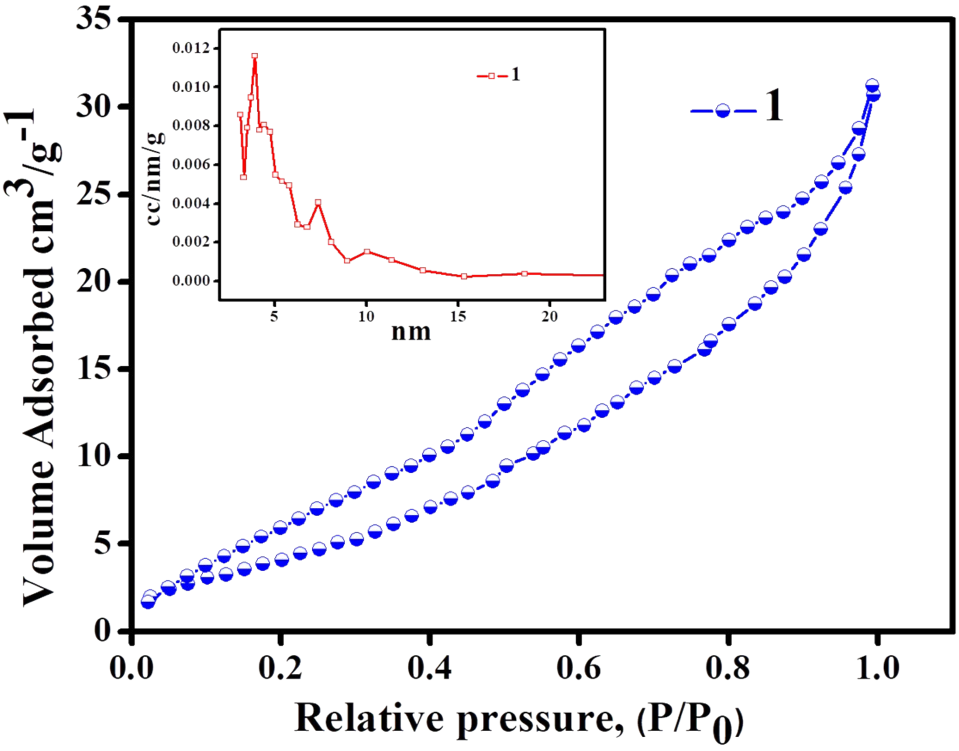

Fig. S5 N_2 isotherm and corresponsing BJH desorption pore size distribution profile of **1**.

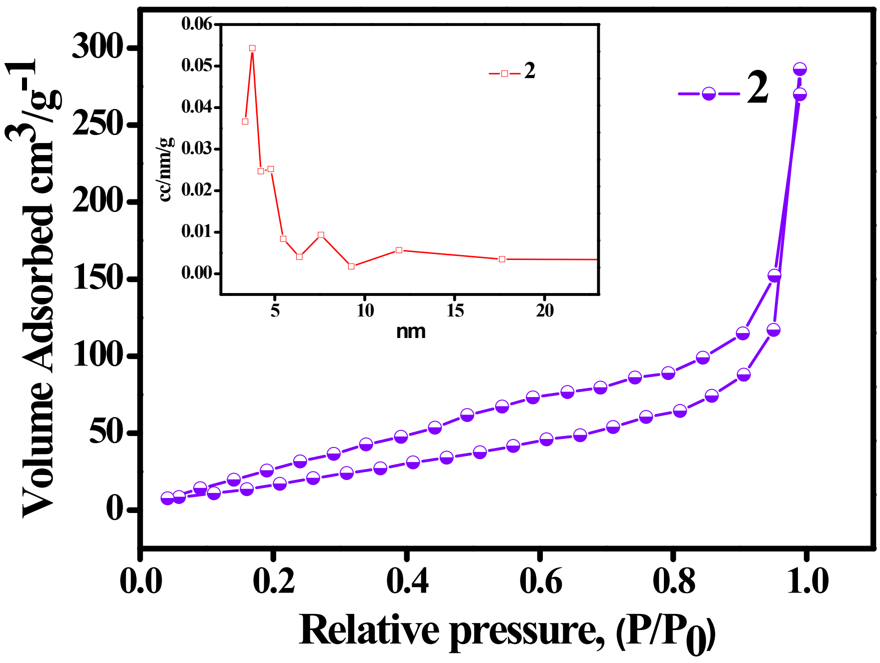

Fig. S6 N_2 isotherm and corresponsing BJH desorption pore size distribution profile of **2.**

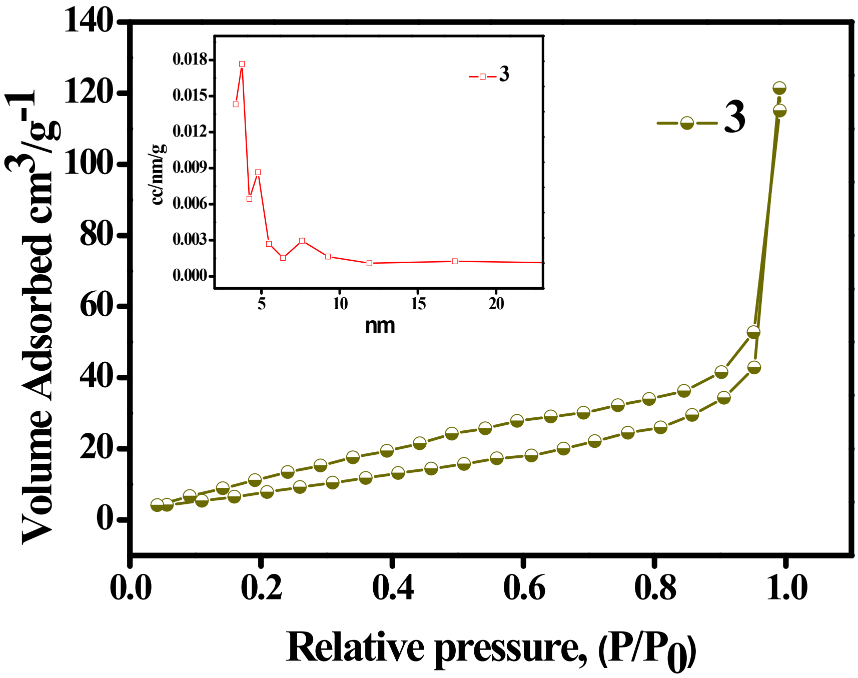

Fig. S7 N_2 isotherm and corresponsing BJH desorption pore size distribution profile of **3.**

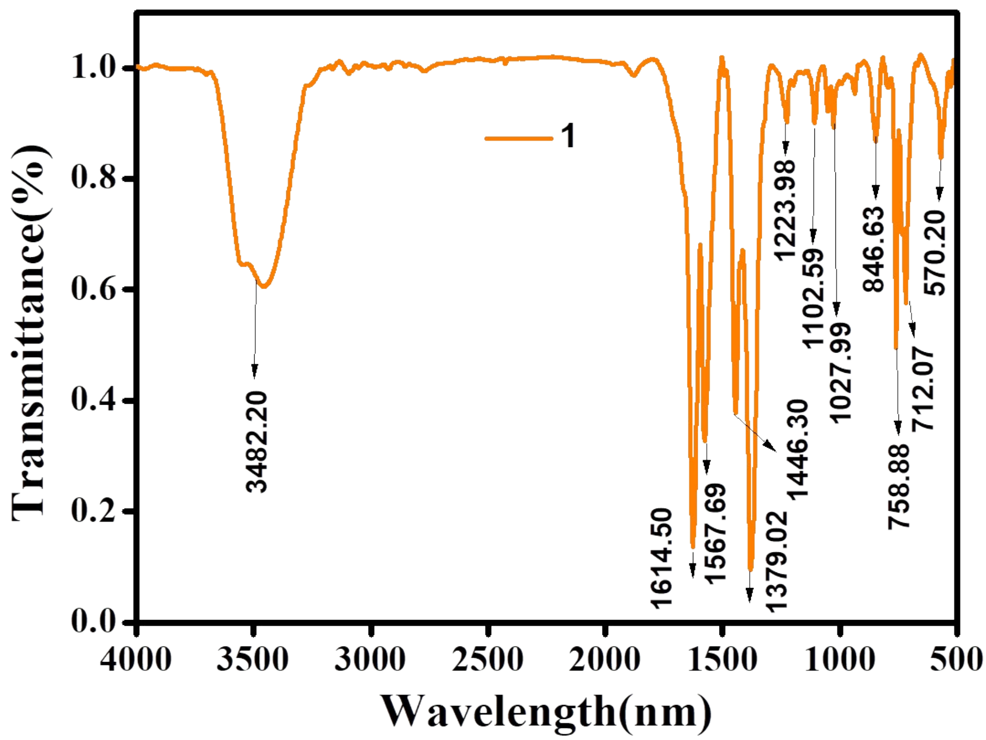

Fig. S8 FT-IR spectrum of **1**.

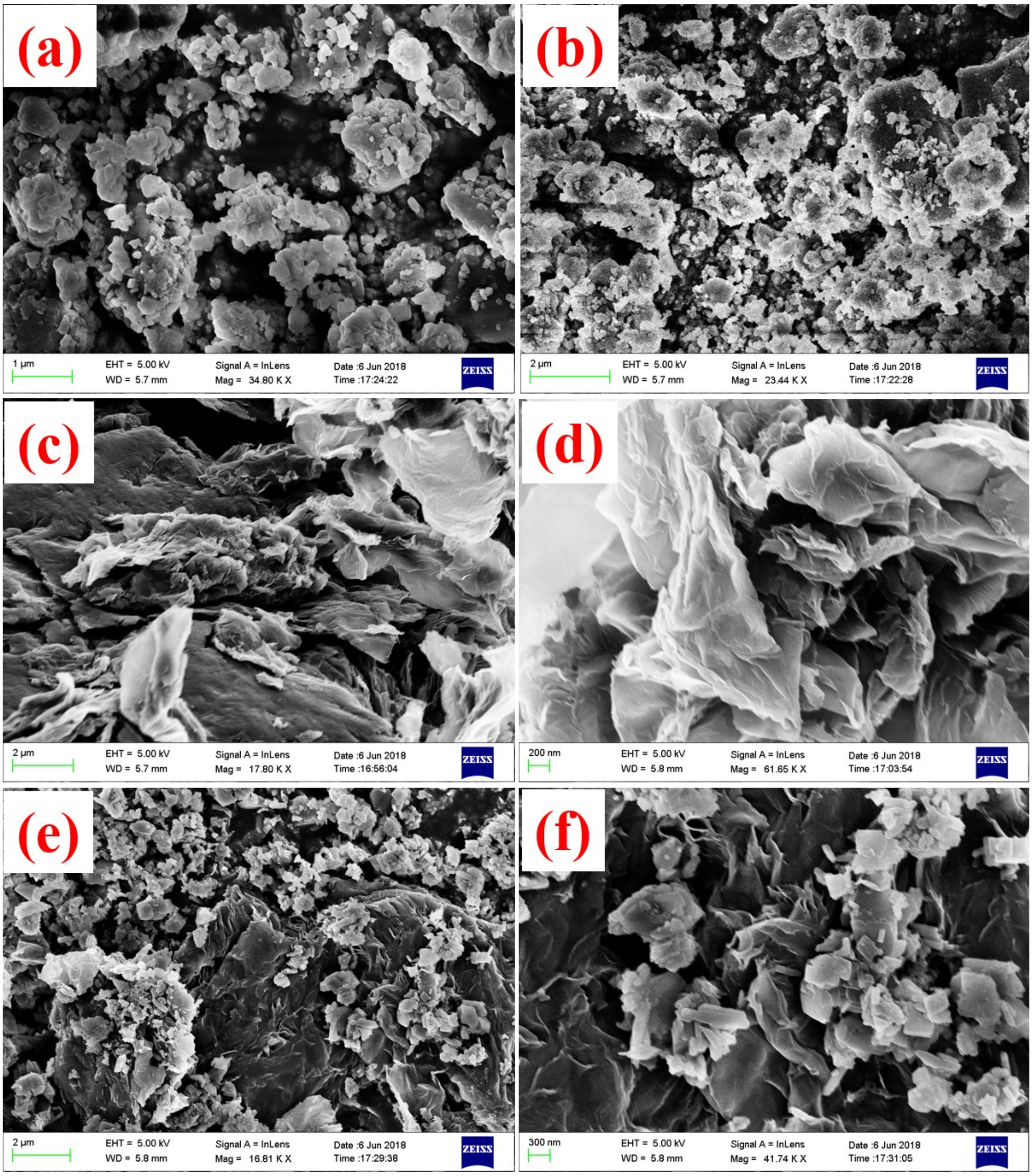

Fig. S9 SEM image of (a,b) **1,** (c,d) **2**, and (e,f) **3**.

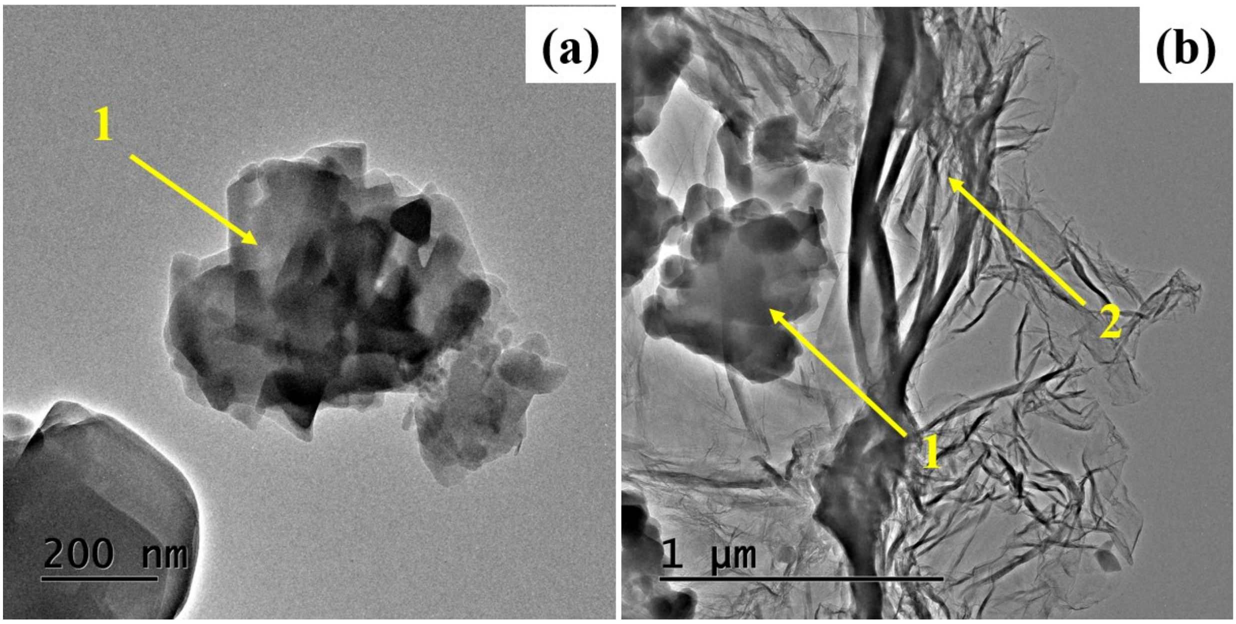

Fig. S10 TEM image of **1** and **3**.

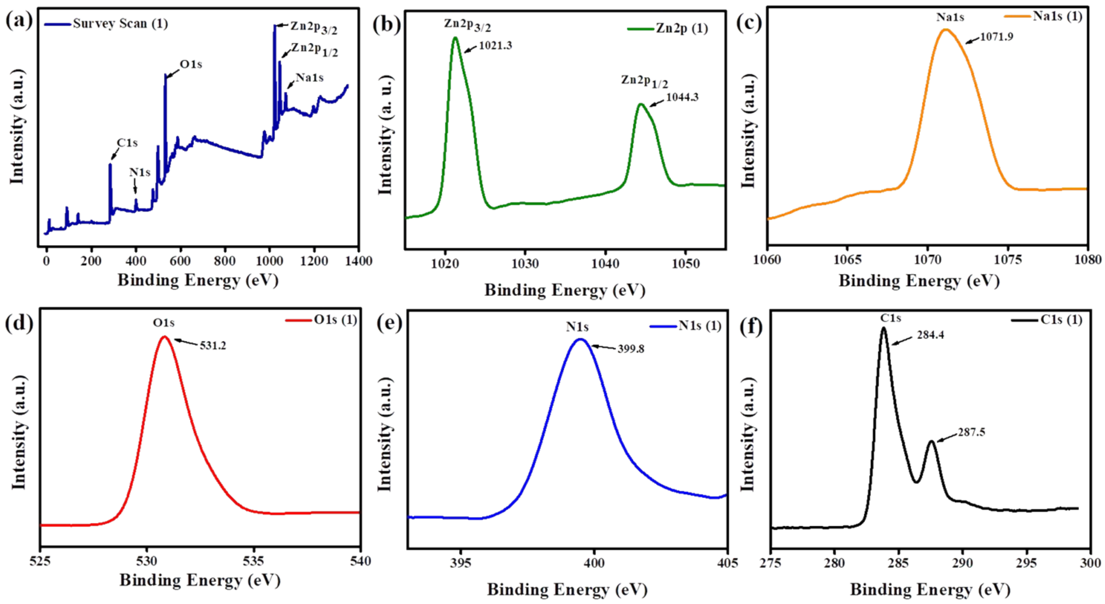

(g)

Peak	Position BE (eV)	Height (CPS)	FWHM (eV)	Area (P) (CPS.eV)	Atomic %
Na 2s	63.16	11881.37	3.13	42050.69	1.93
C 1s	284.47	407853.7	2.46	2026326	54.1
N 1s	399.8	82232.98	3.72	374863.5	6.32
O 1s	531.22	728154.4	3.47	2735869	28.91
Zn2p	1022.03	801948.1	4.4	6024974	8.74

Fig. S11 XPS spectra of **1** (a) survey scan, (b) Zn 2p, (c) Na 1s, (d) O 1s, (e) N 1s, (f) C 1s and (g) Elemental analysis of **1.**

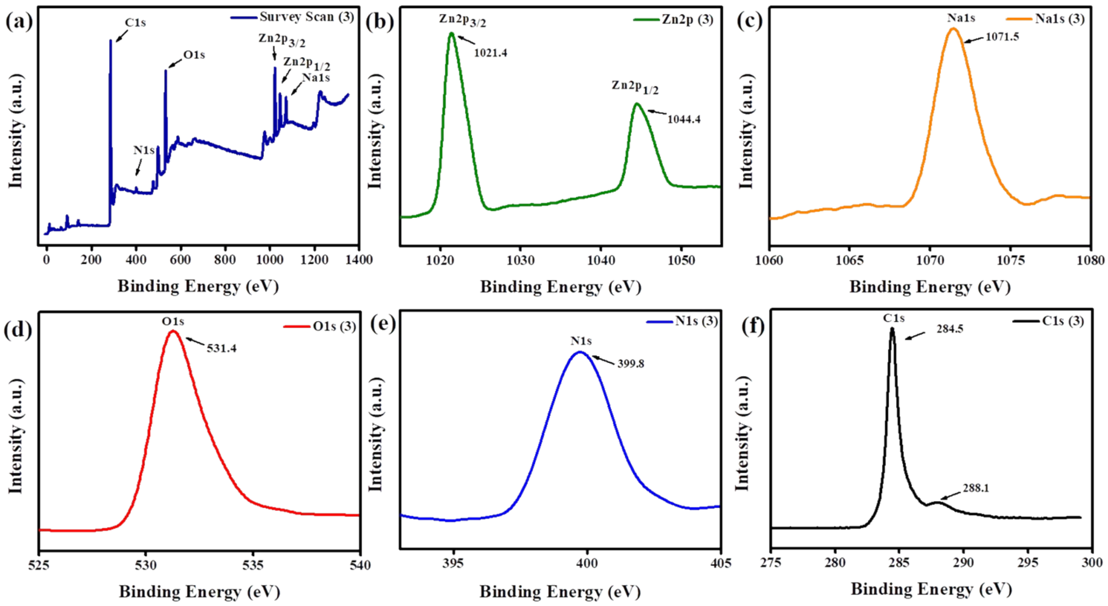

(g)

Peak	Position BE (eV)	Height (CPS)	FWHM (eV)	Area (P) (CPS.eV)	Atomic %
C 1s	284.69	482097	3.69	2163311	76.05
N 1s	399.88	13663.83	4.34	73181.09	1.63
O 1s	531.45	273406.2	4.02	1205291	16.77
Zn 2p	1022.08	183416.8	5.23	1603462	3.06
Na 1s	1071.49	83252.23	3.01	406720.2	2.49

Fig. S12 XPS spectra of **3** (a) survey scan, (b) Zn 2p, (c) Na 1s, (d) O 1s, (e) N 1s, (f) C 1s and (g) Elemental analysis of **3.**

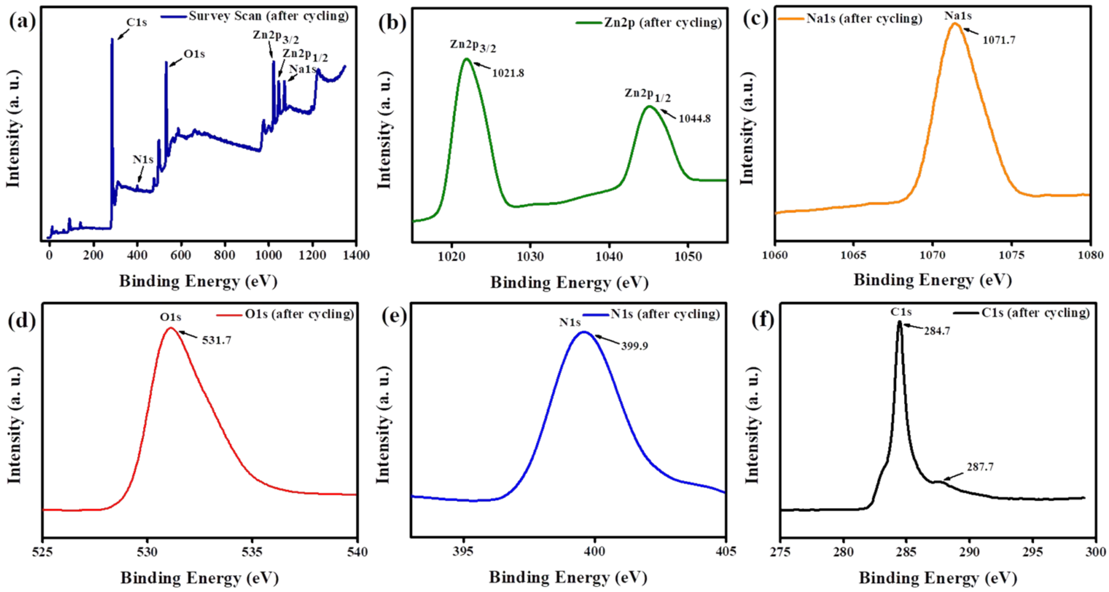

(g)

Peak	Position BE (eV)	Height (CPS)	FWHM (eV)	Area (P) (CPS.eV)	Atomic %
C 1s	284.79	476913.9	3.72	2142535	75.81
N 1s	399.96	13431.21	4.41	72064.33	1.61
O 1s	531.7	263838.4	4.16	1207082	16.9
Zn 2p	1022.18	182012.1	5.25	1596427	3.07
Na 1s	1071.75	80945.31	4.85	422238.2	2.61

Fig. S13 XPS spectra after cycling of **3** (a) survey scan, (b) Zn 2p, (c) Na 1s, (d) O 1s, (e) N 1s, (f) C 1s and (g) Elemental analysis after cycling of **3.**

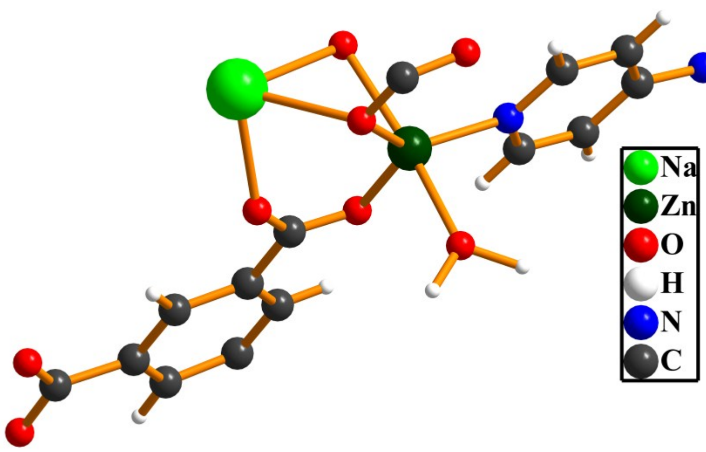

Fig. S14 Assymertic unit of **1**. Color code: Zn (dark green), Na (green), C (dark gray), N (blue), O (red), H (white).

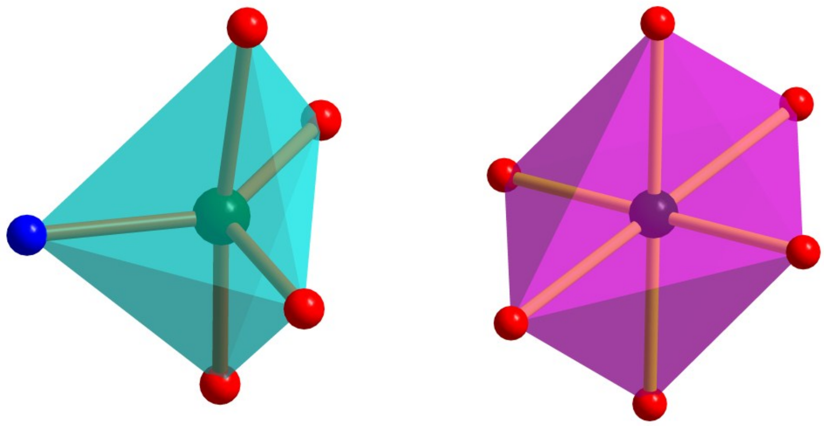

(a) **(b)**

Fig. S15 Distorted trigonal bipyramidal and octahedral co-ordination geometry around (a) Zn(II), and (b) Na(I) ion, present in **1**.

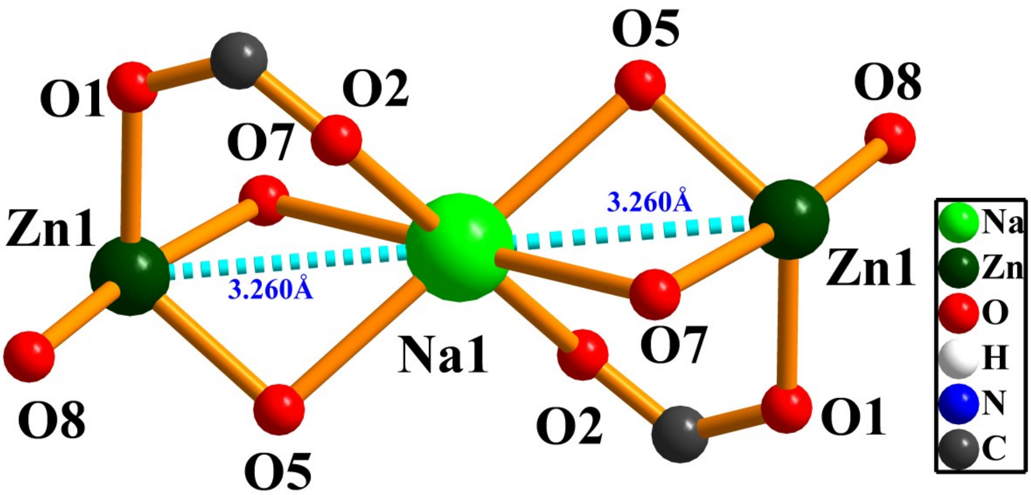

Fig. S16 Representation of $[Zn_2NaO_8]$ cluster in **1**.

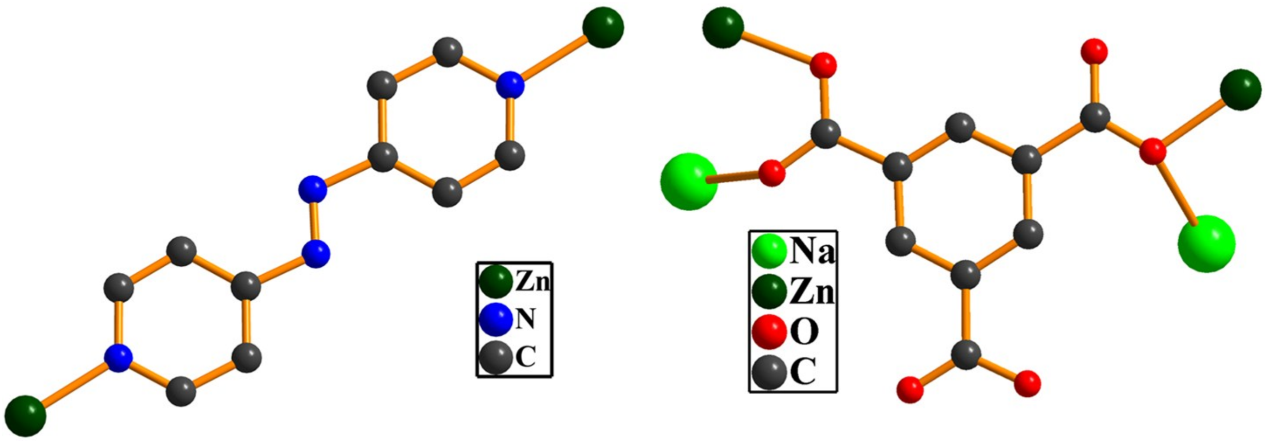

Scheme S1. Coordination modes of ligands in **1**.

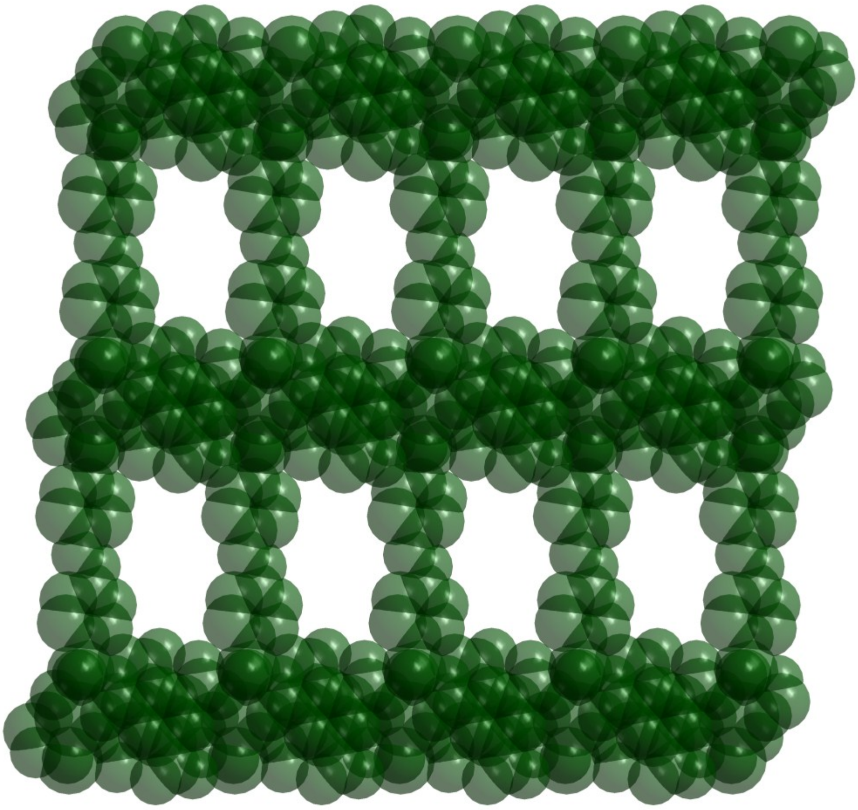

Fig. S17 Space fill model of the 2D framework along *b*-axis in **1**.

CV and GCDs at different ratios

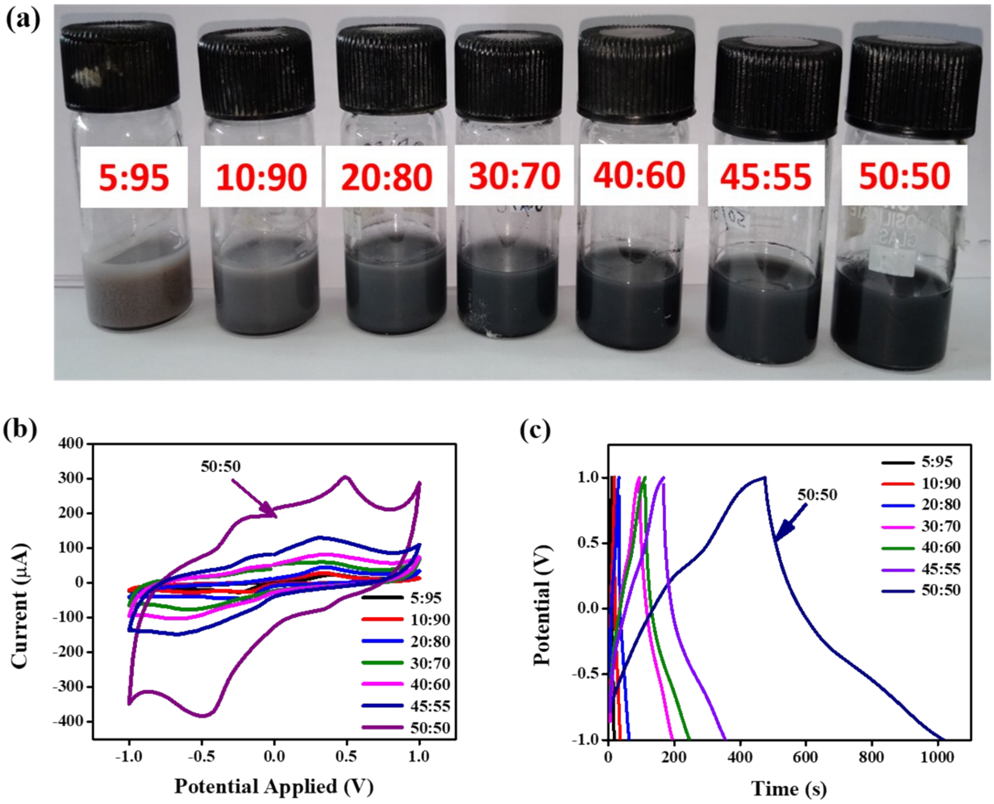

Fig. S18 (a) A series of formed heterostructure **3** at different ratios of **1** and **2**, and (b,c) CV and GCD plots of formed heterostructures of **3** at different ratios of **1** and **2**. (Here. 5:95 indicates 5% of **2** and 95% of **1**, 10:90 indicates 10% of **2** and 90% of **1** and so on...)

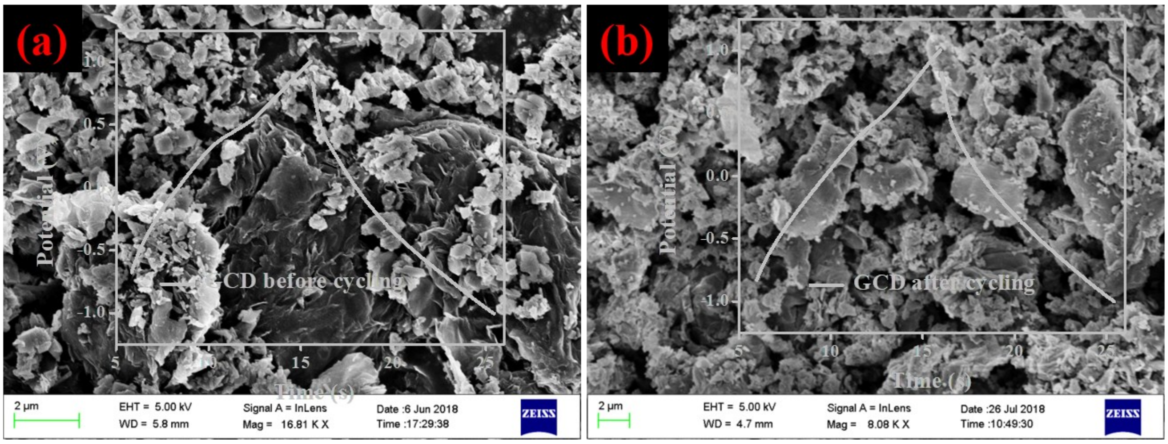

Fig. S19 GCD plots and SEM images of ***3–GCE*** (a) before and (b) after cycling.

The supercapacitor properties of ***3–GCE*** has been analysed at higher mass loading with an effective mass of ~0.25 mg and mass loading of ~3.5 mg/cm^2 in addition to the original mass loading of 0.35 mg/cm^2. The comparison of CV profiles of bare GCE and ***3–GCE*** clearly shows an enhanced CV area and better charge propagation in **3** (Fig. S21a). However, the current response was lesser than that obtained at lower mass loading as shown in Fig. 6c. The CV profiles ware recorded at different scan rates as shown in Fig. S21b. Furthermore, GCD profiles were also recorded at different current densities (Fig. S21c). The discharge time was found to be lesser at each current density compared to that at lower mass loadings (Fig. 7e). The plot between specific capacitance and applied current densities shows a notable decrement in charge storage efficiency w.r.t. increasing current density (Fig. S21d). The maximum specific capacitance obtained was 251.2 F g^{-1} at 1.6 A g^{-1}, which kept on decreasing up to 84 F g^{-1} at 4 A g^{-1}. It was observed that at higher mass loading, specific capacitance decreases, which approves Stoller's findings (*Energy Environ. Sci*., 2010, **3**, 1294–1301), and also in agreement with the general thumb rule that specific capacitance decreases on increasing mass loading.

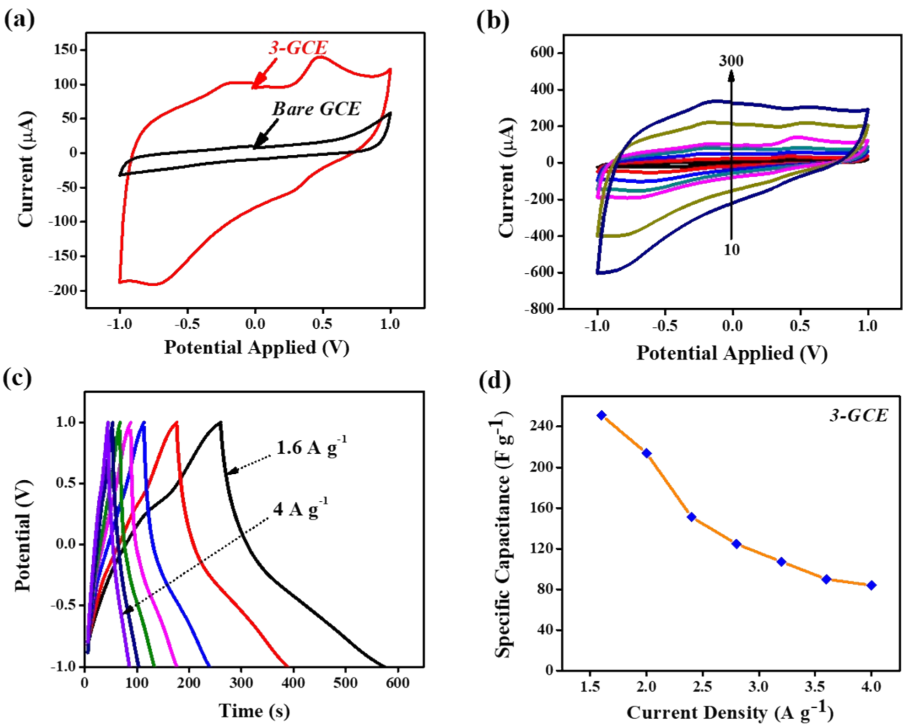

Fig. S20 (a) Comparison of CV profiles of bare GCE and ***3–GCE*** at 100 mV s^{-1}, (b) CV profiles of ***3–GCE*** at varied scan rates (10–300 mV s^{-1}), (c) GCD plots of ***3–GCE*** at different current densities (1.6–4 A g^{-1}), and (d) plot between specific capacitance and current density. (All results at higher mass loading ~3.5 mg/cm^2)

Table S1. Bond lengths [Å] and angles [°] for **1**.

Bond distances	
Na(1) —O(2)	2.292(3)
Na(1) —O(2)#1	2.292(3)
Na(1) —O(5)#1	2.418(3)
Na(1) —O(5)	2.420(3)
Na(1) —O(7)#1	2.505(3)
Na(1) —O(7)	2.505(3)
Na(1) —Zn(1)#1	3.2595(5)
Na(1) —Zn(1)	3.2595(5)
Zn(1) —O(5)	1.991(3)
Zn(1) —O(1)	2.000(3)
Zn(1) —N(1)	2.073(3)
Zn(1) —O(8)	2.098(4)
Zn(1) —O(7)	2.250(3)
Bond angles	
O(5) —Zn(1) —O(1)	124.01(12)
O(5) —Zn(1) —N(1)	136.57(13)
O(1) —Zn(1) —N(1)	98.92(13)
O(5) —Zn(1) —O(8)	89.72(15)
O(1) —Zn(1) —O(8)	93.69(17)
N(1) —Zn(1) —O(8)	94.12(15)
O(5) —Zn(1) —O(7)	83.01(12)
O(1) —Zn(1) —O(7)	87.84(14)
N(1) —Zn(1) —O(7)	93.30(13)
O(8) —Zn(1) —O(7)	172.10(13)
O(5) —Zn(1) —Na(1)	47.67(8)
O(1) —Zn(1) —Na(1)	85.61(9)
N(1) —Zn(1) —Na(1)	143.11(10)
O(8) —Zn(1) —Na(1)	122.27(11)
O(7) —Zn(1) —Na(1)	50.06(8)
O(2) —Na(1) —O(2)#1	180.0
O(2) —Na(1) —O(5)#1	101.26(11)
O(2)#1—Na(1) —O(5)#1	78.74(11)
O(2) —Na(1) —O(5)	78.74(11)
O(2)#1—Na(1) —O(5)	101.26(11)
O(5)#1—Na(1) —O(5)	180.0
O(2) —Na(1) —O(7)#1	93.17(11)
O(2)#1—Na(1) —O(7)#1	86.83(11)
O(5)#1—Na(1) —O(7)#1	69.79(10)

O(5) —Na(1) —O(7)#1	110.21(10)
O(2) —Na(1) —O(7)	86.83(11)
O(2)#1—Na(1) —O(7)	93.17(11)
O(5)#1—Na(1) —O(7)	110.26(10)
O(5) —Na(1) —O(7)	69.79(10)
O(7)#1—Na(1) —O(7)	180.0
O(2) —Na(1) —Zn(1)#1	121.03(8)
O(2)#1—Na(1) —Zn(1)#1	58.97(8)
O(5)#1—Na(1) —Zn(1)#1	37.50(6)
O(5) —Na(1) —Zn(1)#1	142.50(6)
O(7)#1—Na(1) —Zn(1)#1	43.55(7)
O(7) —Na(1) —Zn(1)#1	136.45(7)
O(7) —Na(1) —Zn(1)	43.55(7)
Zn(1)#1—Na(1) —Zn(1)	180.0

Symmetry transformations used to generate equivalent atoms:

#1 -x,-y,-z #2 -x+1,-y+1,-z-2 #3 x+1,y,z #4 x-1,y,z